Materials Chemistry and Physics 240 (2020) 122211

Contents lists available at ScienceDirect

Materials Chemistry and Physics

journal homepage: www.elsevier.com/locate/matchemphys

Dilatometer studies of praseodymium doped ceria: Effect of synthesis methods on sintering behaviour

Irfana Shajahan, Hari Prasad Dasari *, P. Govardhan

Chemical Engineering Department, National Institute of Technology Karnataka, Mangalore, 575025, India

HIGHLIGHTS

- Prepared praseodymium doped ceria (PDC) electrolyte by various synthesis methods.
- MWCOP-ISP PDC sample exhibited uni-modal shrinkage behaviour ($T_{Max} \sim 765\,^{\circ}C$).
- Activation energy of PDC sample by CHR (116 kJ/mol) and Dorn (176 kJ/mol) methods.
- Sintering temperature of PDC sample is decreased to 1100 °C using MWCOP-ISP method.
- Grain boundary diffusion mechanism is obtained for MWCOP-ISP PDC sample.

GRAPHICAL ABSTRACT

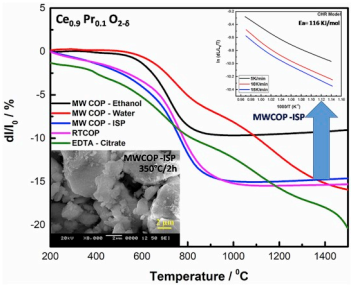

ARTICLE INFO

Keywords:
Praseodymium-doped ceria
Sintering mechanism
Dilatometer
X-ray diffraction
Raman spectroscopy

ABSTRACT

Praseodymium-doped ceria ($Ce_{0.9}Pr_{0.1}O_2$, PDC), as an electrolyte material for IT-SOFCs, is investigated with respect to the effect of synthesis method and a detailed analysis was carried out to understand the effect on crystallite size, morphology, specific surface area and sintering behaviour. The various synthesis routes such as microwave assisted co-precipitation method, room temperature co-precipitation method and EDTA-citrate complexing method was adopted for the synthesis of praseodymium doped ceria-based nano-materials. XRD pattern confirms the fluorite-type crystal structure of ceria and Raman spectroscopy analysis confirms the structure with the presence of oxygen vacancies. PDC synthesised by microwave assisted co-precipitation method using isopropyl alcohol as solvent exhibited better sintering activity, reduced the sintering temperature and promoted the densification rate when compared to other synthesis methods with uni-model shrinkage behaviour with shrinkage maxima at 765 °C. Based on two sintering models (CHR/Dorn method), the initial stage sintering mechanism was investigated in the present study and confirmed that the grain boundary diffusion (m = 2) as the dominant mechanism and the activation energy was found to be 116 kJ/mol (CHR model) and 176 kJ/mol (Dorn Method) for initial stages of sintering for PDC material synthesised by microwave assisted co-precipitation method using isopropyl alcohol as solvent.

1. Introduction

Solid oxide fuel cell (SOFCs) is an electrochemical device that can generate clean and reliable electrical energy using H_2 and O_2 with less environmental impact and higher efficiency. Lowering the operating temperature (600–800 °C) has become increasingly important to

* Corresponding author.
E-mail address: energyhari@nitk.edu.in (H.P. Dasari).

https://doi.org/10.1016/j.matchemphys.2019.122211
Received 5 June 2019; Received in revised form 18 September 2019; Accepted 22 September 2019
Available online 24 September 2019
0254-0584/

enhance the lifetime of SOFCs and to widen the choice of materials for the SOFCs. This would reduce the fabrication cost of SOFC cell, technological and economic problems associated with the components of HT - SOFCs. The electrolyte material of SOFC plays a key role among the different components of SOFC since, it determines the operating temperature of the fuel cell and also prevents the electrical contact of the two electrodes [1]. Lowering the operating temperature of SOFC is important for decreasing the energy consumption, improving the compatibility of materials and to reduce the overall cost.

Ceria-based materials are widely applied in various fields such as oxygen sensors [2], optical devices [3], capacitor devices [4], catalyst [5] and SOFCs [6]. Rare-earth doped ceria-based materials have been considered as good candidates for intermediate temperature (IT-SOFC) and low temperature (LT-SOFC) solid oxide fuel cell electrolyte materials due to their remarkably higher oxide ionic conductivity at lower temperatures than the traditionally used electrolyte material yttria-stabilized zirconia (YSZ) [7,8]. Oxygen vacancies in the CeO_2 lattice when doped with RE elements enhance the redox capability [9], oxygen ion mobility [10,11], thermal stability and oxygen storage capacity (OSC) [12], and have a significant effect on oxide ionic conductivity behaviour [13,14]. It was reported that introduction of praseodymium to a CeO_2 lattice was promising to form oxygen vacancies [15,16]. Among the various trivalent rare earth doped ceria based electrolytes reported in the literature; gadolinium doped ceria and samarium doped ceria form solid solution and introduce oxygen vacancies due to the reduction of Ce^{4+} to Ce^{3+}, which is responsible for better ionic conductivity at a relatively low temperature (600 °C) in these doped samples [17–19]. Over the number of years, detailed investigations of the singly doped ceria electrolytes such as $Ce_{1-x}Gd_xO_{2-y}$ (GDC), $Ce_{1-x}Sm_xO_{2-y}$ (SDC) and $Ce_{1-x}Y_xO_{2-y}$ (YDC) have been extensively carried out. Although there is sufficient literature reported on the different synthesis techniques of Praseodymium doped ceria nano-powder [20–24], only few works has been reported on shrinkage behaviour and decreasing the sintering temperature of $Ce_{1-x}Pr_xO_{2-y}$ (PDC) based electrolyte materials for SOFC applications. It was reported that the ceria praseodymium oxide forms fluorite type solid solution up to 30 mol% PrO_{2-x} for 1550 °C sintered pellet [25] while another study reported that single phase fluorite solid solution is formed up to 35 mol % for 1500 °C sintered pellet [22]. According to our earlier report [16], it was found that 10 mol% PDC synthesised by EDTA-citrate method showed a lower ionic conductivity due to the presence of secondary phase at 1500 °C and exhibited a high sintering temperature of 1500 °C. From these findings, further research was carried out to find suitable synthesis methods for 10 mol% PDC material to reduce the sintering temperature below 1500 °C. Fig. S1 shows that the secondary phase of PDC synthesised by EDTA-citrate method starts at 1000 °C and hence it is mandatory to reduce the sintering temperature below 1000 °C and synthesis approach is followed to overcome the issue. However, there is a lack of information reported on the effect of heat treatment on the solubility of Pr in CeO_2. Therefore, this was the motivation to decrease the sintering temperature below 1000 °C by following different synthesis approach.

Zhang tianshu et al. [26] had found out the sintering mechanism for undoped ceria to be volume diffusion controlled sintering whereas; transition metal oxide doping resulted in the transition of mechanism to viscous flow from volume diffusion. A detailed study on the sintering kinetics for the initial stage of sintering of PDC based materials is reported in the present study. Two different methods (CRH method/Dorn method) have been used in order to calculate the activation energy and to find out the kinetic mechanism in the sintering process. The two different methods that were used for the sintering experiments in the present work are discussed in detail in section 2.

The current research analyses the results of a systematic study of the solubility of 10 mol % Praseodymium doped ceria (10 PDC) solid solutions by using a variant of EDTA – Citrate complexing method at various heat treatment temperatures. The particular composition for this study was chosen based on the previous research work [16]. The purpose of this work is to study the solubility limits of 10 mol% praseodymium doped ceria-based material for SOFCs with the aim to enhance their sintering properties by selecting proper heat treatment conditions and henceforth different synthesis methods were adopted in order to reduce the sintering temperature below the solubility temperature. The different synthesis methods includes microwave assisted co-precipitation method using ethanol, water and isopropyl alcohol as solvents, room temperature co-precipitation method using isopropyl alcohol and EDTA citrate method were denoted as MWCOP- Ethanol, MWCOP- Water, MWCOP- ISP, RTCOP and EDTA- Citrate respectively in the following sections of the present study. The main objective of the present study is to calculate the activation energy and the sintering mechanism of the as-prepared sample which exhibits a good sintering activity as compared to the other synthesis methods/samples. The as-prepared samples were characterized using XRD analysis, Raman Spectroscopy analysis and Scanning electron microscopy analysis.

2. Methods used to calculate the activation energy of sintering

The two different models that are used for calculating the activation energy and the sintering mechanism are (1) constant heating rate method and (2) Dorn method.

2.1. Constant heating rate method

Woolfrey and bannister [27] had developed an equation for the isothermal initial stage of sintering and based on the developed equation, Young and Cutler [28] have developed an equation which can be applied to constant heating rate conditions as follows:

$$\frac{\left(\Delta L/L_0\right)}{T} = A_1\, exp\left(\frac{-Q}{(m+1)RT}\right) \tag{1}$$

Taking natural logarithm on both sides, equation (1) reduces to

$$\ln\left(\frac{\Delta L/L_0}{T}\right) = lnA_1 - \frac{Q}{(m+1)R}\frac{1}{T} \tag{2}$$

where, R is the universal gas constant, the exponent m depends on the mechanism of sintering; m = 0 indicates viscous flow, m = 1 indicates volume diffusion and m = 2 indicates grain boundary diffusion [26]. Therefore the apparent activation energy, Q from equation (2) can be calculated under CHR conditions from the slope of ln [($\Delta L/L_0$)/T] vs. (1/T) with a slope [–Q/(m+1)R] by determining the value of m. The value of m can be obtained by performing constant heating rate experiments at different heating rates reported by Woolfrey et al. and a relationship between fractional shrinkage and heating rate was established [27].

$$\left(\Delta L/L_0\right)_T = A_2 C^{\frac{-1}{(m+1)}} \tag{3}$$

Taking the natural logarithmic of relative shrinkage vs. heating rate yields a slope of magnitude 1/(m+1). Alternatively, Q can be found out.

2.2. Dorn Method

In this method, the apparent activation energy for the initial stage of sintering was determined by giving a rapid heating rate from one isothermal range to another isothermal range so that the microstructure of the sample remains the same [29]. The equation used to determine the apparent activation energy is expressed as follows:

$$Q = \frac{RT_1T_2}{(T_2 - T_1)}\ln\left[\left(dY/dt\right)_2/\left(dY/dt\right)_1\right] \tag{4}$$

The present investigation compares the controlled heating rate experiments with that of Dorn's method. The sintering mechanism along with the activation energy was estimated using the CRH models and the Dorn method.

3. Experimental

3.1. Sample preparation

Different solvents such as ethanol, water, isopropyl alcohol were used for the investigation of the formation of PDC by using microwave assisted co-precipitation method. Stoichiometric amounts of cerium nitrate hexahydrate (SRL Chemicals >99%) and Praseodymium nitrate hexahydrate (Sigma Aldrich Chemicals 99%) were dissolved in different solvents (Loba chemicals 99%). Ammonium hydroxide (25% ammonia spectrum reagents) was added dropwise to the mixture to maintain a pH of ~9. The solution was then collected and microwaved at a temperature of 150 °C and a power of 540 W for 30 min. The gel was then dried at 120 °C for 24 h. The obtained powder was calcined at 450 °C/2 h for ethanol and water; 350 °C/2 h for isopropyl alcohol sample. In room temperature co-precipitation synthesis of PDC powder, the gel obtained was dried at room temperature for 72 h.

$Ce_{0.9}Pr_{0.1}O_{2-\delta}$ was prepared by EDTA- Citrate complexing method to find out the solubility temperature reported in the present study as reported elsewhere [30]. In a typical preparation, the chemicals used are Praseodymium nitrate hexahydrate ($Pr(NO_3)_3{\cdot}6H_2O$, Sigma Aldrich Chemicals 99%), Cerium nitrate hexahydrate ($Ce(NO_3)_3{\cdot}6H_2O$, SRL Chemicals ≥99%), EDTA (ethylenediamine-tetraacetic acid, Sigma Aldrich Chemicals ≥99%) and citric acid (Sigma Aldrich Chemicals ≥99%), Ammonium hydroxide (Spectrum reagents). Ethylene diamine tetra acetic acid and citric acid monohydrate are used as chelating agents. The mole ratio of total metal ions to EDTA and citric acid used was 1:1:1.5. The obtained solid black precursor after the oven drying at 150 °C/24 h is then ground and calcined at 600 °C/5 h to obtain the Praseodymium doped ceria sample. The obtained sample is then calcined at 800 °C, 900 °C, 1000 °C, 1100 °C and 1200 °C in air for 5 h and the physical characterization of the as-synthesised samples were carried out to study the solubility of praseodymium in ceria.

3.2. Sample characterization

X-ray diffractions (XRD) patterns were collected on an XPERT Pro diffractometer using Cu Kα radiation ($\lambda = 0.1540$ nm). The working voltage of the instrument was 40 kV and the working current was 30 mA in the 2θ range of 20°–80° with a step size of 0.02 and the time for the step is 2s. The lattice parameter and the average crystallite size of the sample were determined by using full-width half maximum of the most prominent XRD peak by using the Debye–Scherer equation. Raman measurements were performed on a Bruker (Alpha) KBr/ATR in the range of 375–7500 cm^{-1} with KBr Optics and high sensitivity DLATGS. Scanning electron microscopy/Energy dispersive spectroscopy (SEM/EDS) analysis was done by using JSM 6380LA.

3.3. Sintering studies experimental procedure

The PDC powder was uniaxially pressed (150 MPa) to form green pellets with a diameter of 10 mm and thickness of 12 mm. To determine the activation energy, constant heating rate (CHR) sintering experiments was performed by using a dilatometer (Netzsch, DIL 402, Germany) at three different heating rates of 5, 10, 15 K/min from 30 °C to 1500 °C/30 min in air after which the samples were cooled down to the room temperature. The densities of the sintered samples were measured by Archimedes' method.

The isothermal experiments were conducted by heating the sample to the desired temperature at a higher heating rate so that the microstructure of the sample remains unchanged (i.e., 500 - 730 °C), and then held at this temperature for about 30 min and then cooled down to room temperature.

4. Results and discussions

4.1. X-ray diffraction and Raman Spectroscopy analysis

The decomposition of PDC black precursor synthesised by MWCOP-Ethanol, MWCOP- Water, MWCOP- ISP, RTCOP and EDTA- Citrate method was analysed by Thermogravimetric analysis before calcination (see Fig. S2 (a)–(e)). This confirms that complete decomposition of all the impurities occurs below 450 °C for MWCOP- Ethanol and MWCOP-water; 350 °C for MWCOP- ISP and RTCOP; 400 °C for EDTA- Citrate method; and these temperatures are used for the calcination of the corresponding samples for 2 h in air.

Fig. 1(a) and Fig. 1(b) represents the XRD diffraction pattern and FT - Raman spectra with an excitation laser line (785 nm) of PDC powders synthesised by microwave assisted co-precipitation method (Ethanol, water and iso-Propyl alcohol as solvents), room temperature co-precipitation method (Iso-Propyl alcohol as solvent) and EDTA- Citrate method respectively. XRD patterns of all the as-prepared powder confirms the single phase and the peaks can be indexed to the (111), (200), (220), (311), (222), (400) and (331) planes with a typical cubic fluorite-type crystalline structure of pure CeO_2 [21,31]. No additional secondary peaks corresponding to praseodymium oxide were identified in all the samples which indicate the complete incorporation/substitution of praseodymium oxide into the lattice of CeO_2 and the complete formation of single phase ceria praseodymium solid solution with the mentioned elements [32]. Raman analysis confirms the sharp and intense first order peak at 465 cm^{-1} which is due to the F_{2g} symmetric mode of fluorite type cubic structure of pure CeO_2, which corresponds to the vibration of oxygen ions around cerium ions [16,33] (Please see supplementary information for more details).

4.2. SEM analysis

The representative SEM micrograph of PDC sample synthesised by various methods are shown in Fig. 2 (a)-(e). It can be seen from the figures that sponge-like agglomerated (hard agglomerates) structures are observed for PDC sample synthesised by MWCOP- Water and EDTA-Citrate method which could hinder the densification during sintering process. The SEM image of MWCOP (ethanol and isopropyl alcohol as solvents) and room temperature COP appeared to consist of weak agglomerates, which could result in a higher sintering activity when compared to the former samples. Table S1 (see supplementary data) shows the EDX analysis of PDC powders which confirmed the presence of Ce, Pr and O in the composition.

4.3. Dilatometer studies

The linear shrinkage and shrinkage rate behaviour of PDC powders obtained from dilatometer studies as a function of temperature at a constant heating rate of 5 K/min are depicted in Fig. 3(a) and Fig. 3(b) respectively. Interestingly, Fig. 3(a) clearly shows that the synthesis method has a profound effect in shifting the onset of the sintering temperature from a higher range to a lower temperature (from ~600 °C for EDTA- Citrate method to ~350 °C for MWCOP- ISP), and significantly enhances the densification phenomena. Most importantly, it has been reported that smaller crystallite size and particle size of the powder could be the reason for such phenomena [34]. The smallest crystallite size shown by PDC powder synthesised by EDTA Citrate method (see Table 1) also had an early onset of sintering but did not achieve full density at 1500 °C. The reason for this type of behaviour of the sample may be due to the presence of high degree of agglomerates in the starting powder.

MWCOP- ISP and RTCOP reached a maximum linear shrinkage of

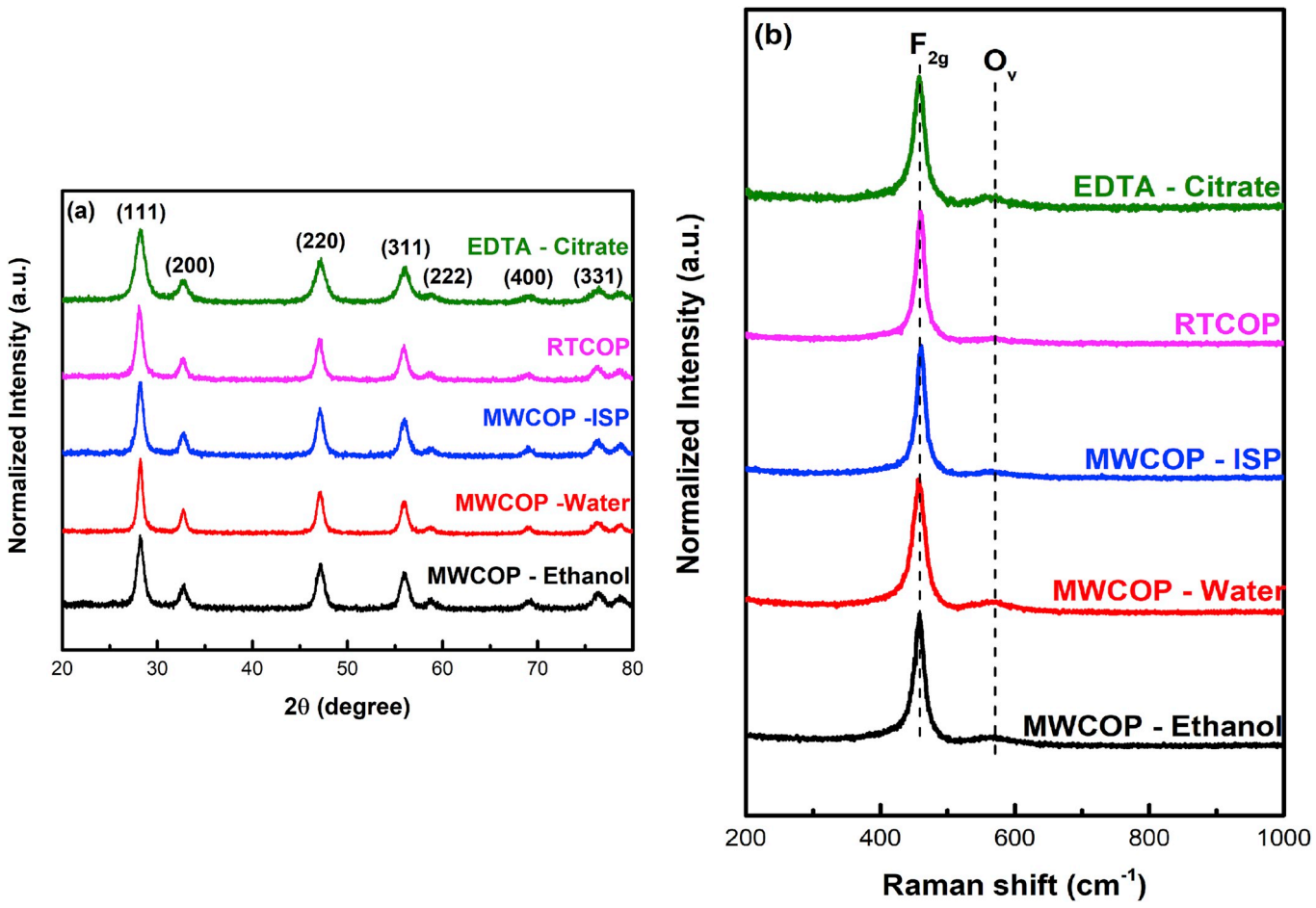

Fig. 1. (a) XRD pattern of PDC samples synthesised by microwave assisted co-precipitation method, room temperature co-precipitation method and EDTA-citrate method. (b) Raman spectra of PDC samples synthesised by microwave assisted co-precipitation method, room temperature co-precipitation method and EDTA-citrate method.

~16% at a shrinkage temperature of 900 °C, whereas MWCOP- Ethanol has reached a line shrinkage of ~9% at 900 °C. The maximum linear shrinkage of 15% was achieved for MWCOP- ISP and 16% for RTCOP below 900 °C, which indicates that the full densification of the powder can be attained below 900 °C. The shrinkage of MWCOP- Ethanol began at 600 °C and is saturated at 900 °C with a single shrinkage maxima at 730 °C. As discussed earlier, the monomodal pore size distribution obtained in the three as-prepared samples indicates the uniform pore population within the compacted powder structure due to the fracturing of agglomerates and the uniform distribution of the same [35]. The rearrangement and the fracturing of the agglomerates results in the high densification of the sample prepared [35]. The pressure applied on the powder should be more than the agglomerate strength inorder to achieve a high green density of the compact, vice-versa results in a bimodal pore size distribution of the sample. Thus the soft agglomerate powder with a uniform pore size distribution results in a single peak in the first derivative shrinkage curve (shrinkage rate curve). Thus the homogeneous pore size distribution of the present investigation indicates the high sinterability of the as-prepared powders. Table 1 summarises the results of sintering experiments of the powders synthesised by different methods.

It can be seen from Fig. 3(b) that the sintering process of the samples and the temperature of maximum shrinkage rate of as prepared PDC powder changes with the effect of synthesis methods and is in the following order T_{Max}^{RTCOP} (~775 °C)> $T_{Max}^{MWCOP-ISP}$ (~765 °C) >$T_{Max}^{MWCOP-Water}$ (~750 °C,1200 °C)>$T_{Max}^{MWCOP-Ethanol}$ (~730 °C)>$T_{Max}^{EDTA\ Citrate}$ (~700 °C,1150 °C). The sintering of MWCOP-Water and EDTA- Citrate showed a multiple shrinkage behaviour, which can be attributed to different size distribution of the agglomerates or due to different particle/pore size distribution, with the shrinkage maxima at (750 °C, 1200 °C) and (700 °C,1150 °C) respectively. The sintering of MWCOP- Ethanol, MWCOP- ISP and RTCOP exibited a single maximum shrinkage or an uni modal agglomerate size distribution indicating a single densification mechanism is occurring in the samples. It can be seen from Table 1, that the temperature of the maximum shrinkage rate was lowered from ~1200 °C for MWCOP- Water to less than ~800 °C for MWCOP- ISP, MWCOP- Ethanol and RTCOP.

The density achieved for the MWCOP- ISP in the present study was superior to that of the density obtained by the earlier experiment (EDTA-Citrate method) in our previous work [16]. The high surface area of MWCOP- ISP and RTCOP provide the driving force for sintering and result in an increase in the shrinkage rate [36]. During the sintering process, PDC sample synthesised by MWCOP- ISP exibited maximum shrinkage. However, it is likely that the high sinterability of as-prepared MWCOP- ISP suggest the feasibility of using PDC as an electrolyte material for IT-SOFCs and hence PDC synthesised by microwave assisted co-precipitation method using iso-propyl alcohol has been chosen for studying the sintering mechanism and kinetic parameters, which is discussed in detail in section 4.4.

Fig. 4 shows the XRD pattern of MWCOP- Ethanol, MWCOP- ISP and RTCOP sample sintered at 1100 °C/2 h and MWCOP- Water and EDTA-Citrate sintered at 1450 °C/2 h. The sintering temperature is fixed from the results obtained for dilatometer studies. It can be seen that the peaks of the sintered samples become narrower when compared to the

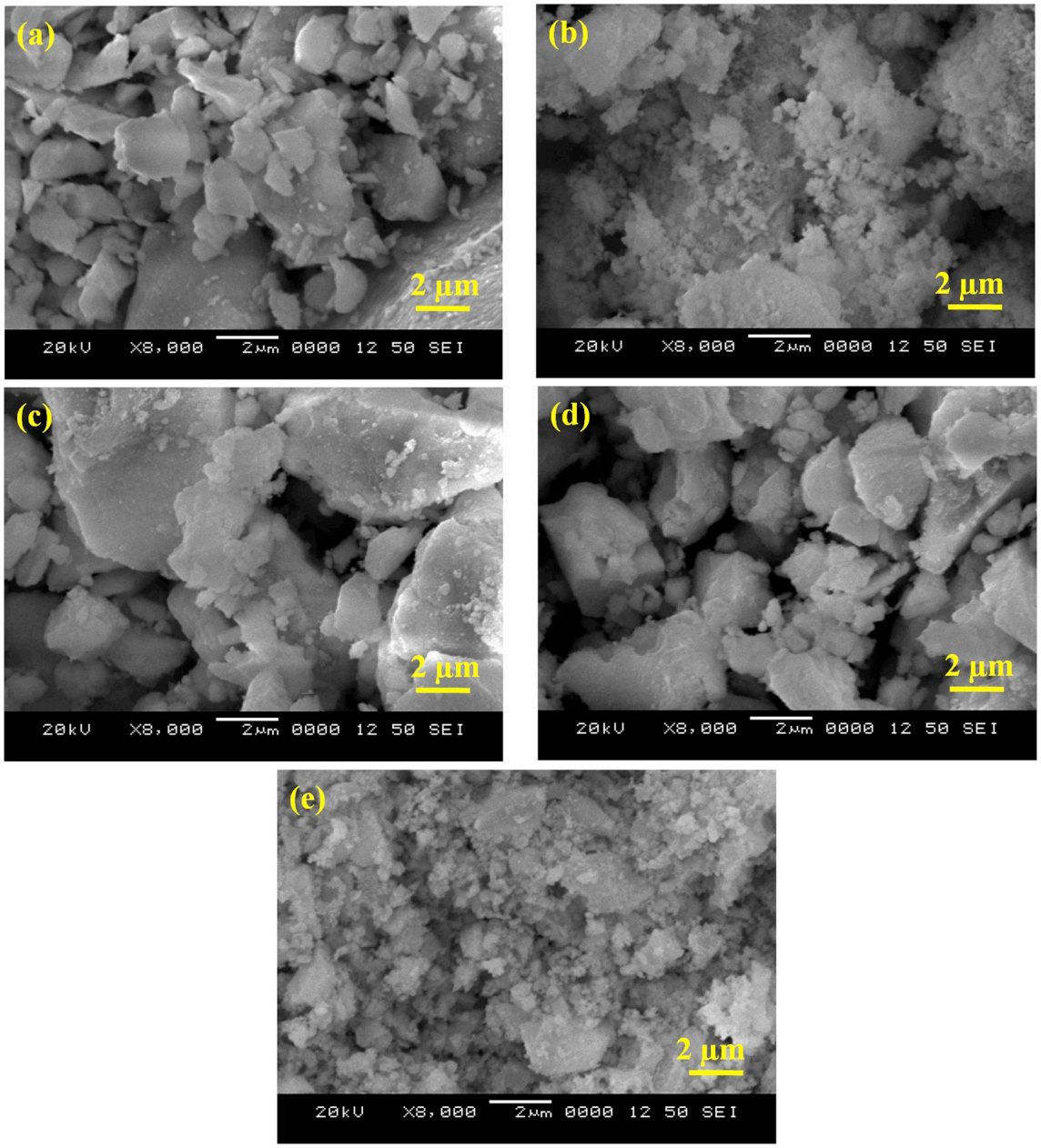

Fig. 2. SEM micrograph of PDC samples synthesised by microwave assisted co-precipitation method, room temperature co-precipitation method and EDTA-citrate method.

calcined samples due to the increase in the mean crystalline size with the increase in the heat treatment temperature [37]. It can be seen from the figure that with the increase in the sintering temperature the width of the XRD peaks gradually decreases.

The SEM images of sintered pellets obtained at 1100 °C/2 h from MWCOP- Ethanol, MWCOP- ISP and RTCOP sample; and 1450 °C/2 h from MWCOP- Water and EDTA- Citrate are shown in Fig. 5 (a)–(e). PDC synthesised by MWCOP- ISP (Fig. 5c) exhibit a better sintering properties with a relative density of 94% at a lower temperature of 1100 °C/2 h compared to MWCOP- Ethanol (Fig. 5a) and RTCOP (Fig. 5d) sintered at the same temperature and are in good agreement with the relative density measured through Archimedes' principle mentioned in Table 1. The difference in the relative density can be due to the difference in the synthesis method and the microstructural changes which can be observed from Fig. 5. As seen, the SEM morphology of the PDC sample synthesised by MWCOP- Water (Fig. 5b) and EDTA- Citrate method (Fig. 5e) confirmed a lower densification and the density was around 90% even after sintering at 1450 °C/2 h due to the incomplete sintering or due to the residual porosity. Meanwhile, the amount of porosity decreased with the effect of synthesis methods was very pronounced and no micro-cracks or macro-cracks are found in any of the sintered samples of MWCOP-Ethanol, MWCOP-ISP and RTCOP but in the case of MWCOP-Water and EDTA-Citrate sample even after sintering to a higher temperature of 1450 °C resulted in a porous sample.

MWCOP- ISP appear quite dense without any noticeable connected pores with a very uniform microstructure compared to the other samples which indicate the formation of a typical sintered ceramic compact/dense bulk PDC material and these results further supports the linear shrinkage behaviour (See Fig. 3a). Eventually, it was hard to find pores on MWCOP- ISP sample sintered at 1100 °C; whereas many pores still existed in the samples sintered at 1450 °C. The calculated relative densities from Archimedes method for the PDC sintered pellet from MWCOP-Ethanol, MWCOP-water, MWCOP-ISP, RTCOP and EDTA-citrate are 88%, 90%, 94%, 91% and 90% of the theoretical value

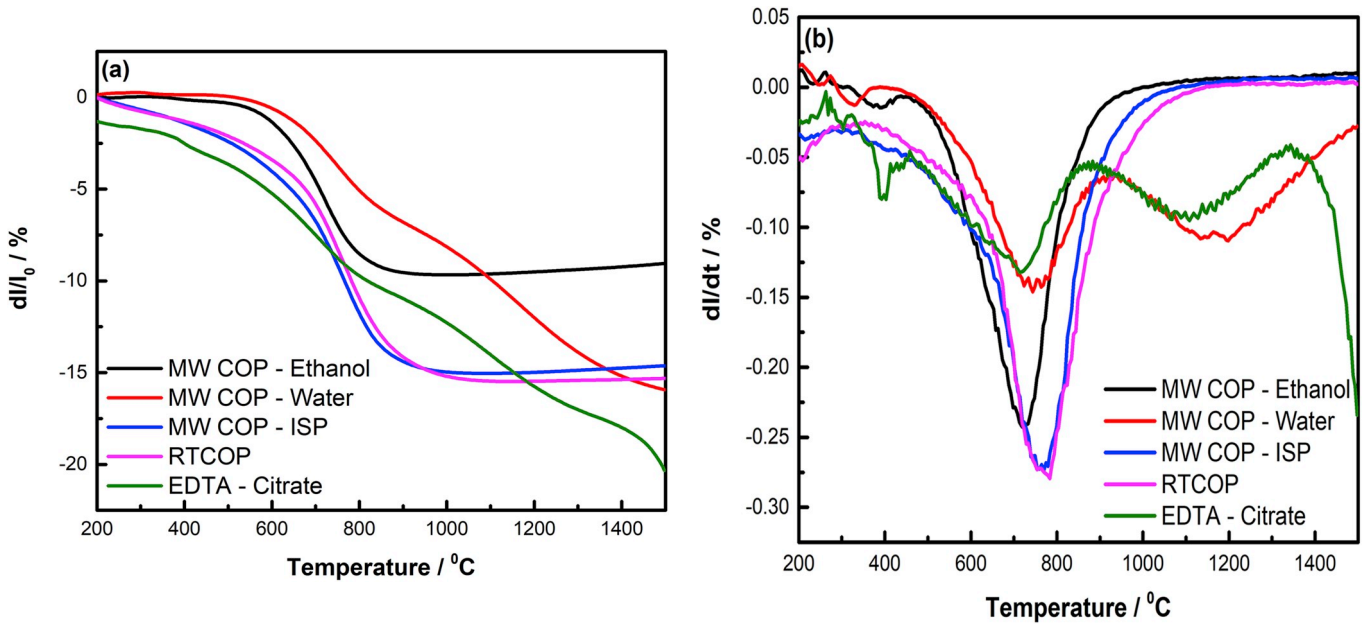

Fig. 3. (a) Linear shrinkage of PDC green pellets from 200 °C to 1500 °C. (b) Shrinkage rate of PDC green pellets from 200 °C to 1500 °C.

Table 1
Comparison of 10-mol% PDC material synthesised by various methods.

Synthesis method		Crystallite size (nm)	Lattice Constant (Å)	BET Surface area (m^2/g)	Calcination Temperature (°C)	Initial sintering temperature (°C)	Sintering end temperature (°C)	Maximum shrinkage rate temperature (°C)	Sintering Temperature (°C)/2 h	Relative Density (%)
MWCOP	Ethanol	9.2	5.47	61	450/2 h	505	895	730	1100	88
	Water	12.2	5.47	50	450/2 h	584	>1500	750, 1200	1450	90
	Iso-Propyl Alcohol	9.6	5.47	71	350/2 h	429	956	765	1100	94
Room temperature co-precipitation method		9.7	5.49	73	350/2 h	432	1040	775	1100	91
EDTA - Citrate		6.6	5.47	82	400/2 h	365	>1500	700, 1150	1450	90

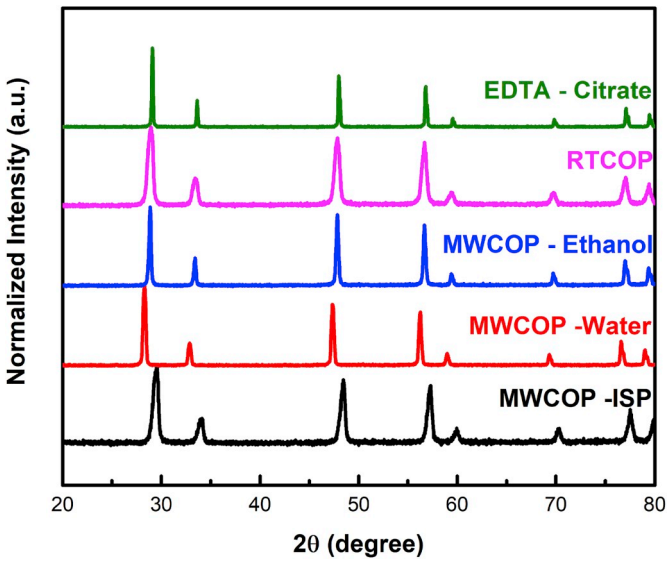

Fig. 4. XRD pattern of sintered PDC pellet synthesised by microwave assisted co-precipitation method, room temperature co-precipitation method and EDTA-citrate method.

respectively. The obtained result indicates that MWCOP- ISP is suitable as solid electrolytes by decreasing the sintering temperature to1100 °C.

4.4. Sintering kinetic data studies (CHR method)

Fig. 6 shows the plot of the natural logarithm of ($\Delta L/L_0$) and heating rate (C) at a particular temperature based on equation (3). The average value of [1/(m+1)] from the slope at different temperatures are listed in Table 2. The average value of m for praseodymium doped ceria has been found out to be 2.04. From the value of (m), it is evident that the sintering rate controlling mechanism in PDC is grain boundary diffusion for the initial stages of sintering. Lahiri et al. [38] had reported that grain boundary diffusion dominates the sintering mechanism when the particle size is small in the case of ceramics and crystalline materials. As a result, the smaller particles will result in a faster neck to neck growth which is the driving force for grain boundary diffusion to takes place in the early stages of sintering.

The apparent activation energy of the PDC material synthesised by microwave assisted co-precipitation method using iso-propyl alcohol as solvent has been calculated from the plot of $\ln((\Delta L/L_0)/T)$ vs. (1/T) by taking the average of the three slopes is shown in Fig. 7. The interval of the shrinkage has been taken for linear parts of the curves which indicates only one sintering mechanism during the early stages of sintering [26]. The apparent activation energy of the 10 mol% PDC material synthesised by microwave assisted co-precipitation method using

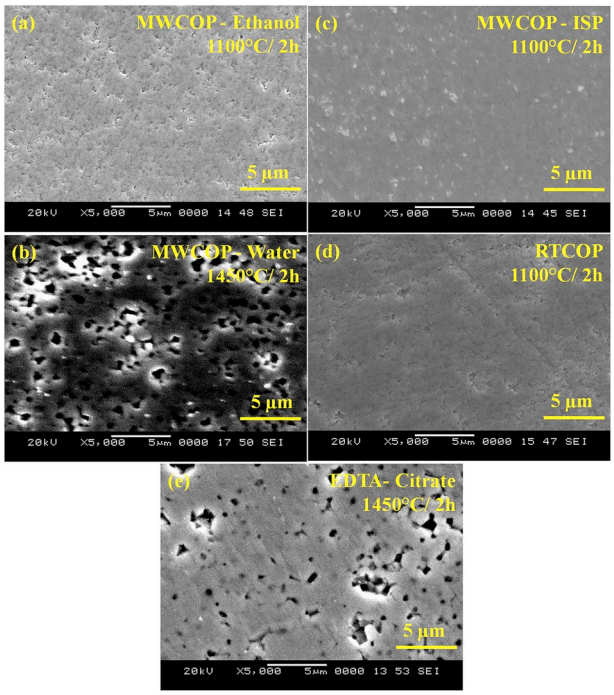

Fig. 5. SEM micrograph of sintered PDC pellet synthesised by microwave assisted co-precipitation method, room temperature co-precipitation method and EDTA-citrate method.

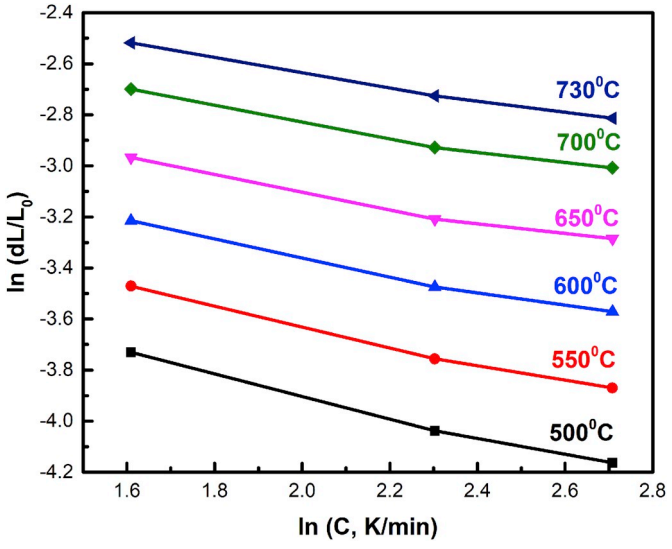

Fig. 6. The natural logarithm of $\ln(\Delta L/L_0)$ versus ln(C) for 10 mol% PDC of MWCOP-ISP.

Table 2
The value of 1/(m+1) at different temperatures of MWCOP-ISP PDC pellet.

Temp (°C)	500	550	600	650	700	730
10 PDC 1/(m+1)	0.399	0.368	0.331	0.295	0.287	0.285

iso-propyl alcohol as solvent is found to be 116 kJ/mol. The activation energy obtained for 10 PDC for the early stage of sintering is much lower than that of gadolinium doped ceria in reducing atmosphere (290 ± 20 kJ/mol) [39].

Chen et al. [40] had reported that grain boundary diffusion governs the densification of pure ceria whereas, He et al. [39] reported that in a reducing atmosphere lattice diffusion dominate the early stage sintering of gadolinium doped ceria (10GDC). In the present work, PDC exhibit the same sintering mechanism on the densification as that reported by Chen et al. for pure ceria.

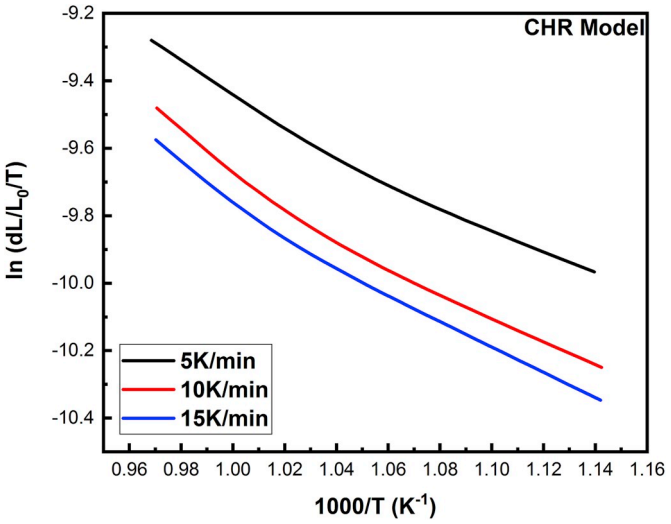

Fig. 7. Plot of ln $((\Delta L/L_0)/T)$ versus 1/T for 10 mol% PDC of MWCOP-ISP.

4.5. Sintering kinetic data studies (Dorn Method)

The isothermal shrinkage to calculate the apparent activation energy from the Dorn method was done in the interval of 550–750 °C at 50 °C interval. The activation energy of PDC material synthesised by microwave assisted co-precipitation method using iso-propyl alcohol as solvent was calculated using equation (4) and was found to be 176 kJ/mol.

The sintering temperature obtained for the electrolyte material synthesised by microwave assisted co-precipitation method using iso-propyl alcohol ($Ce_{0.9}Pr_{0.1}O_2$) as solvent has been decreased from 1500 °C (PDC synthesised by EDTA-Citrate method) of our previous work. This result showed that $Ce_{0.9}Pr_{0.1}O_2$, the sintering temperature of PDC material can be further reduced to use as an electrolyte material in low operating temperature SOFC electrolytes. Our future work would be positioned on how to further decrease the sintering temperature of PDC based material by co-doping chemistry with transition metal oxides to a lower value than that obtained by the present synthesis method (Microwave assisted co-precipitation method using iso-propyl alcohol as solvent, <900 °C) and to check the ionic conductivity will be the topic of the forth coming paper.

5. Conclusion

Praseodymium-doped ceria-based electrolyte materials for SOFCs were prepared and studied by different synthesis methods such as microwave assisted co-precipitation method using ethanol, water and isopropyl alcohol as solvents, room temperature co-precipitation method using isopropyl alcohol and EDTA citrate method. In $Ce_{0.9}Pr_{0.1}O_2$, the solid solution solubility of Pr in CeO_2 extends to 1000 °C. All the samples exhibited a cubic fluorite-type crystal structure of CeO_2 from XRD analysis. The crystallite size of PDC material was in the range of 6–12 nm. In comparison to other synthesis methods, PDC synthesised by MWCOP- ISP exhibited better sintering activity with a temperature of maximum shrinkage rate at the temperature of ~765 °C. Two different sintering models (CHR/Dorn method) have been used to study the kinetics and the sintering parameters of MWCOP- ISP system. The activation energy for the initial stages of sintering was in the range of 116 kJ/mol (CHR model) and 176 kJ/mol (Dorn Method). It has been

identified that grain boundary diffusion is the dominating mechanism for early stages of sintering. The results suggest that PDC based material prepared by MWCOP –ISP may be a better electrolyte material for IT-SOFCs.

Authors' contribution

IS obtained all the experimental data and contributed to material synthesis. HPD conceived the study. IS, HPD and GP analysed all the experimental data, and all the authors contributed to writing and editing the document.

Acknowledgements

This work was supported by DST-SERB-Early Career Research Award (Grant No. ECR/2016/002010ES). One of the authors (IS) would like to thank NITK for giving the opportunity to do PhD with a full scholarship. We would like to thank DST and Materials research centre at Malaviya National Institute of Technology (MNIT) Jaipur for providing Raman data using FT-Raman spectrometer (Bruker FRS) instrument and Manipal Institute of technology (MIT) Manipal for providing the XRD results. We would like to thank National Institute of Technology, Surathkal (NITK) for providing SEM/EDX data.

Appendix A. Supplementary data

Supplementary data to this article can be found online at https://doi.org/10.1016/j.matchemphys.2019.122211.

Nomenclature

m	Sintering Parameter
Q	Activation energy (KJ/mol)
R	Universal gas constant
Y	Shrinkage
$(\Delta L/L_0)$	Relative Shrinkage
ΔL	Total shrinkage, L_0 - L_t
L_0	Initial length of the sample
L_t	Length of the sample at time t
T	Absolute Temperature
t	Time
C	Heating rates
A_1, A_2	Constant depending on sintering mechanisms and material parameters
(dY/dt)	Rate of shrinkage

References

[1] A.B. Stambouli, E. Traversa, Solid oxide fuel cells (SOFCs): a review of an environmentally clean and efficient source of energy, Renew. Sustain. Energy Rev. 6 (2002) 433–455, https://doi.org/10.1016/S1364-0321(02)00014-X.
[2] N. Izu, N. Murayama, W. Shin, I. Matsubara, S. Kanzaki, Resistive oxygen sensors using cerium oxide thin films prepared by metal organic chemical vapor deposition and sputtering, Jpn. J. Appl. Phys. 43 (2004) 6920–6924, https://doi.org/10.1143/JJAP.43.6920. Part 1.
[3] C. Kaittanis, S. Santra, A. Asati, J.M. Perez, A cerium oxide nanoparticle-based device for the detection of chronic inflammation via optical and magnetic resonance imaging, Nanoscale 4 (2012) 2117, https://doi.org/10.1039/c2nr11956k.
[4] C.H. Cheng, H.H. Hsu, W.B. Chen, A. Chin, F.S. Yeh, Characteristics of cerium oxide for metal–insulator–metal capacitors, Electrochem. Solid State Lett. 13 (2010) H16, https://doi.org/10.1149/1.3258042.
[5] S.M. Vickers, R. Gholami, K.J. Smith, M.J. MacLachlan, Mesoporous Mn- and La-doped cerium oxide/cobalt oxide mixed metal catalysts for methane oxidation, ACS Appl. Mater. Interfaces 7 (2015) 11460–11466, https://doi.org/10.1021/acsami.5b02367.
[6] D.H. Prasad, J.W. Son, B.K. Kim, H.W. Lee, J.H. Lee, Synthesis of nano-crystalline Ce0.9Gd0.1O1.95 electrolyte by novel sol-gel thermolysis process for IT-SOFCs, J. Eur. Ceram. Soc. 28 (2008) 3107–3112, https://doi.org/10.1016/j.jeurceramsoc.2008.05.021.
[7] J.W. Fergus, Electrolytes for solid oxide fuel cells, J. Power Sources 162 (2006) 30–40, https://doi.org/10.1016/j.jpowsour.2006.06.062.
[8] R.O. Fuentes, R.T. Baker, Synthesis and properties of Gadolinium-doped ceria solid solutions for IT-SOFC electrolytes, Int. J. Hydrogen Energy 33 (2008) 3480–3484, https://doi.org/10.1016/j.ijhydene.2007.10.026.
[9] K. Krishna, A. Bueno-López, M. Makkee, J.A. Moulijn, Potential rare earth modified CeO2 catalysts for soot oxidation. I. Characterisation and catalytic activity with O2, Appl. Catal. B Environ. 75 (2007) 189–200, https://doi.org/10.1016/j.apcatb.2007.04.010.
[10] S. Piñol, M. Morales, F. Espiell, Low temperature anode-supported solid oxide fuel cells based on gadolinium doped ceria electrolytes, J. Power Sources 169 (2007) 2–8, https://doi.org/10.1016/j.jpowsour.2007.01.039.
[11] M. Mogensen, N.M. Sammes, G.A. Tompsett, Physical, chemical and electrochemical properties of pure and doped ceria, Solid State Ion. 129 (2000) 63–94, https://doi.org/10.1016/S0167-2738(99)00318-5.
[12] A.P. Anantharaman, H.P. Dasari, J.H. Lee, H. Dasari, G.U.B. Babu, Soot oxidation activity of redox and non-redox metal oxides synthesised by EDTA–citrate method, Catal. Lett. 147 (2017) 3004–3016, https://doi.org/10.1007/s10562-017-2181-7.
[13] H. Yahiro, Y. Eguchi, K. Eguchi, H. Arai, Oxygen ion conductivity of the ceria-samarium oxide system with fluorite structure, J. Appl. Electrochem. 18 (1988) 527–531, https://doi.org/10.1007/BF01022246.
[14] H.L. Tulleh, A.S. Nowick, Doped ceria as a solid oxide electrolyte, J. Electrochem. Soc. 122 (1975) 255–259.
[15] S. Rossignol, C. Descorme, C. Kappenstein, D. Duprez, Synthesis, structure and catalytic properties of Zr–Ce–Pr–O mixed oxides, J. Mater. Chem. 11 (2001) 2587–2592, https://doi.org/10.1039/b102763h.
[16] I. Shajahan, J. Ahn, P. Nair, S. Medisetti, S. Patil, V. Niveditha, G. Uday Bhaskar Babu, H.P. Dasari, J.H. Lee, Praseodymium doped ceria as electrolyte material for IT-SOFC applications, Mater. Chem. Phys. 216 (2018) 136–142, https://doi.org/10.1016/j.matchemphys.2018.05.078.
[17] H. Inaba, H. Tagawa, Ceria-based solid electrolytes, Solid State Ion. 83 (1996) 1–16.
[18] B.C.H. Steele, Appraisal of Ce1−yGdyO2−y/2 electrolytes for IT-SOFC operation at 500°C, Solid State Ion. 129 (2000) 95–110, https://doi.org/10.1016/S0167-2738(99)00319-7.
[19] H. Yahiro, K. EGUCHI, H. ARAi, Electrical properties and reducibilities of ceria-rare earth oxide systems and their application to solid oxide fuel cell, Solid State Ion. 36 (1989) 71–75, https://doi.org/10.1016/0167-2738(89)90061-1.
[20] P. Shuk, M. Greenblatt, Hydrothermal synthesis and properties of mixed conductors based on Ce1−xPrxO2−δ solid solutions, Solid State Ion. 116 (1999) 217–223, https://doi.org/10.1016/S0167-2738(98)00345-2.
[21] A.I.Y. Tok, S.W. Du, F.Y.C. Boey, W.K. Chong, Hydrothermal synthesis and characterization of rare earth doped ceria nanoparticles, Mater. Sci. Eng. A 466 (2007) 223–229, https://doi.org/10.1016/j.msea.2007.02.083.
[22] M.-J. Chen, S. Cheng, F.-Y. Wang, J.F. Lee, Y.L. Tai, Study of Pr-doped ceria-based electrolytes for ITSOFC, ECS Trans. 7 (2007) 2245–2252, https://doi.org/10.1149/1.2729341.
[23] C. Esther Jeyanthi, R. Siddheswaran, P. Kumar, M. Karl Chinnu, K. Rajarajan, R. Jayavel, Investigation on synthesis, structure, morphology, spectroscopic and electrochemical studies of praseodymium-doped ceria nanoparticles by combustion method, Mater. Chem. Phys. 151 (2015) 22–28, https://doi.org/10.1016/j.matchemphys.2014.10.001.
[24] M. Guo, J. Lu, Y. Wu, Y. Wang, M. Luo, UV and Visible Raman Studies of Oxygen Vacancies in Rare-Earth-Doped Ceria, 2011, pp. 3872–3877.
[25] M. Nauer, B.C.H. Steele, An evaluation of Ce-Pr oxides and Ce-Pr-Nb oxides mixed conductors for cathodes of solid oxide fuel Cells : structure , thermal expansion and electrical conductivity, J. Eur. Ceram. Soc. 14 (1994) 493–499.
[26] Tianshu Zhang, Peter Hing, Haitao Huang, Early-stage sintering mechanisms of Fe-doped CeO2, J. Mater. Sci. 37 (2002), 1997–1003, 10.1023/A.
[27] J.L. Woolfrey, M.J. Bannister, Nonisothermal techniques for studying initial-stage sintering, J. Am. Ceram. Soc. 55 (1972) 390–394.
[28] W.S. Young, I.B. Cutler, Initial sintering with constant rates of heating, J. Am. Ceram. Soc. 53 (1970) 659–663, https://doi.org/10.1111/j.1151-2916.1970.tb12036.x.
[29] J.J. Bacmann, G. Cizeron, Dorn method in the study of initial phase of uranium dioxide sintering, J. Am. Ceram. Soc. 51 (1968) 209–212, https://doi.org/10.1111/j.1151-2916.1968.tb11874.x.
[30] D.H. Prasad, S.Y. Park, E.O. Oh, H. Ji, H.R. Kim, K.J. Yoon, J.W. Son, J.H. Lee, Synthesis of nano-crystalline La1-xSrxCoO 3-δ perovskite oxides by EDTA-citrate complexing process and its catalytic activity for soot oxidation, Appl. Catal. Gen. 447–448 (2012) 100–106, https://doi.org/10.1016/j.apcata.2012.09.008.
[31] M. Jamshidijam, R.V. Mangalaraja, A. Akbari-Fakhrabadi, S. Ananthakumar, S. H. Chan, Effect of rare earth dopants on structural characteristics of nanoceria synthesized by combustion method, Powder Technol. 253 (2014) 304–310, https://doi.org/10.1016/j.powtec.2013.10.032.
[32] K. Kuntaiah, P. Sudarsanam, B.M. Reddy, A. Vinu, Nanocrystalline Ce1-xSmxO2-δ (x = 0.4) solid solutions: structural characterization versus CO oxidation, RSC Adv. 3 (2013) 7953–7962, https://doi.org/10.1039/c3ra23491f.
[33] K. Ahn, D.S. Yoo, D.H. Prasad, H. Lee, Y. Chung, J. Lee, Role of multivalent Pr in the formation and migration of oxygen vacancy in Pr-doped ceria: experimental and first-principles investigations, Chem. Mater. 24 (2012) 4261–4267.
[34] D.H. Prasad, J.H. Lee, H.W. Lee, B.K. Kim, J.S. Park, Correlation between the powder properties and sintering behaviors of nano-crys-talline gadolinium-doped ceria, J. Ceram. Process. Res. 11 (2010) 523–526.
[35] A. Ghosh, A.K. Suri, B.T. Rao, T.R. Ramamohan, Synthesis of nanocrystalline sinteractive 3Y-TZP powder in presence of ammonium sulphate and poly ethylene

glycol, Adv. Appl. Ceram. 108 (2008) 183–188, https://doi.org/10.1179/174367608x353629.
[36] T. Selvaraj, B. Johar, S.F. Khor, Iron/zinc doped 8 mol% yttria stabilized zirconia electrolytes for the green fuel cell technology: a comparative study of thermal analysis, crystalline structure, microstructure, mechanical and electrochemical properties, Mater. Chem. Phys. 222 (2019) 309–320, https://doi.org/10.1016/j.matchemphys.2018.10.019.
[37] L. XU, A. SHUI, W. DAI, Study on the preparation and structure of nanocrystal-based Sm^{3+}-doped ceria, J. Ceram. Soc. Japan. 123 (2015) 443–447, https://doi.org/10.2109/jcersj2.123.443.
[38] D. Lahiri, S.V.R. Rao, G.V.S.H. Rao, R.K. Srivastava, Study on sintering kinetics and activation energy of UO2 pellets using three different methods, J. Nucl. Mater. 357 (2006) 88–96, https://doi.org/10.1016/j.jnucmat.2006.05.046.
[39] Z. He, H. Yuan, J.A. Glasscock, C. Chatzichristodoulou, J.W. Phair, A. Kaiser, S. Ramousse, Densification and grain growth during early-stage sintering of Ce0.9Gd0.1O1.95-δ in a reducing atmosphere, Acta Mater. 58 (2010) 3860–3866, https://doi.org/10.1016/j.actamat.2010.03.046.
[40] P.L. Chen, I.W. Chen, Sintering of fine oxide powders: II, sintering mechanisms, J. Am. Ceram. Soc. 80 (1997) 637–645, https://doi.org/10.1111/j.1151-2916.1997.tb02879.x.